

EUROPEAN ORGANIZATION FOR NUCLEAR RESEARCH

CERN - AB Department

CERN-AB-2006-040

**ESTIMATION OF DECAY LOSSES AND DYNAMIC VACUUM FOR THE
BETA-BEAM ACCELERATOR CHAIN**

M. Benedikt, A. Fabich, M. Kirk¹⁾, C. Omet¹⁾, P.Spiller¹⁾

CERN, Geneva, Switzerland

Abstract

The Beta-beam is based on the acceleration and storage of radioactive ions. Due to the large number of ions required and their relatively short lifetime, beam losses are a major concern. This paper estimates the decay losses for the part of the accelerator chain comprising the CERN PS and SPS machines. For illustration purposes, the power deposition in these accelerators is compared to that expected for nominal CNGS proton operation. The effect of the beam losses on the dynamic vacuum is simulated and the consequences for machine operation are discussed.

¹⁾ GSI, Darmstadt

Presented at
EPAC'06, Edinburgh, UK, June 26-30, 2006

*Geneva, Switzerland
June 2006*

ESTIMATION OF DECAY LOSSES AND DYNAMIC VACUUM FOR THE BETA-BEAM ACCELERATOR CHAIN*

M. Benedikt[#], A. Fabich, CERN, Geneva, Switzerland
M. Kirk, C. Omet, P. J. Spiller, GSI, Darmstadt, Germany

Abstract

The beta-beam is based on the acceleration and storage of radioactive ions. Due to the large number of ions required and their relatively short lifetime, beam losses are a major concern. This paper estimates the decay losses for the part of the accelerator chain comprising the CERN PS and SPS machines. For illustration purposes, the power deposition in these accelerators is compared to that expected for nominal CNGS proton operation. The beam losses induced vacuum dynamics is simulated and the consequences for machine operation are discussed.

BETA-BEAM BASELINE SCENARIO

The beta-beam neutrino source is based on the decay of beta-active isotopes stored in a high energy decay ring [1]. The beta-beam task within the EURISOL DS [2] is studying an accelerator baseline scenario [3], where the major boundaries are:

- to reach an annual flux of $2.9 \cdot 10^{18}$ anti-neutrinos or $1.1 \cdot 10^{18}$ neutrinos per physics year of 10^7 s [4]; and
- to use the existing PS and SPS at CERN for the acceleration to the top energy at $\gamma=100$ for both ions.

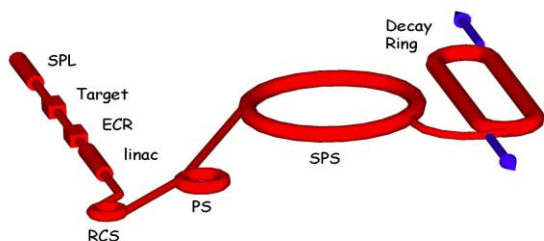


Figure 1: Schematic layout of the beta-beam complex.

The ions of choice are ${}^6\text{He}$ (electron anti-neutrino emitter) and ${}^{18}\text{Ne}$ (electron neutrino emitter). Their half-lives at rest are $t_{1/2}({}^6\text{He}) = 0.81$ s and $t_{1/2}({}^{18}\text{Ne}) = 1.67$ s. Isotopes are produced by a primary proton beam (e.g. SPL) impinging on a target. These drift into an ECR, where they are partly or fully stripped. Post-acceleration is done by a linac and a Rapid Cycling Synchrotron (RCS), which all need to be designed. Further acceleration of fully stripped ions is achieved using the existing PS and SPS machines. The isotopes are finally

* We acknowledge the financial support of the European Community under the FP6 "Research Infrastructure Action - Structuring the European Research Area" EURISOL DS Project Contract no. 515768 RIDS. The EC is not liable for any use that can be made on the information contained herein.

[#] Michael.Benedikt@cern.ch

injected into the decay ring (to be designed [5]) using asymmetric bunch merging [6] and stored for the production of the useful neutrino beam (Figure 1).

The Cycle of Accumulation and Acceleration

The acceleration cycle for the Beta-beam baseline accelerator complex is shown in Figure 2 for ${}^6\text{He}$ and in Figure 3 for ${}^{18}\text{Ne}$.

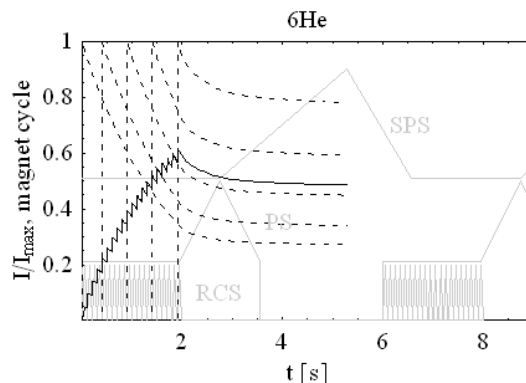


Figure 2: Cycle of the Beta-beam complex accelerating ${}^6\text{He}$. For illustration purposes the single bunch intensities (dashed) are indicated for the 1st, 5th, 10th, 15th and 20th bunch.

Source, post-accelerator and RCS are operated at 10 Hz. Twenty RCS bunches are accumulated at injection energy in the PS over 1.9 s. The beam is then accelerated in PS and SPS to $\gamma=100$. The black solid line indicates the total beam intensity during the acceleration cycle, where the time of accumulation is clearly visible as a saw tooth pattern. The magnet cycles of the RCS, PS and SPS are superimposed (grey line).

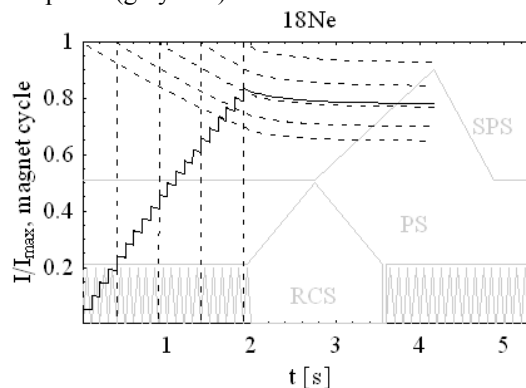


Figure 3: Cycle of the Beta-beam complex accelerating ${}^{18}\text{Ne}$ (see also Figure 2).

During the long accumulation in the PS at low gamma and the following acceleration at low gamma, the intensity of the bunches decreases remarkably due to

decay losses. All single bunch intensities are normalized to the equivalent intensity at injection to the PS.

Decay losses

The parent particle population as a function of time during accumulation, acceleration and storage decreases as $dN(t)/dt = -\ln(2)/(t_{1/2} * \gamma(t)) * N(t)$, where $\gamma(t)$ is the usual relativistic parameter. The decay products are ${}^6\text{Li}$ for ${}^6\text{He}$ and ${}^{18}\text{F}$ for ${}^{18}\text{Ne}$, with a decay branching ratio of unity in both cases. With the ions fully stripped (atomic number A , charge Q , specific momentum p), the decay changes the charge-to-mass ratio. Therefore the magnetic rigidity $B\rho = A/Q * p$ increases by a factor 1.5 for the ${}^6\text{He}$ case and decreases by 10% for the ${}^{18}\text{Ne}$ case and the daughter particles are lost.

Table 1: Ion rates averaged over the beta-beam cycle

Rate [s^{-1}]	${}^6\text{He}$	${}^{18}\text{Ne}$
RCS	$3.1 * 10^{12}$	$1.5 * 10^{12}$
PS	$1.9 * 10^{12}$	$1.3 * 10^{12}$
SPS	$1.5 * 10^{12}$	$1.2 * 10^{12}$

The decay losses during acceleration require increased injection intensities at the different stages of the accelerator chain. Table 1 summarizes the ion rates at injection averaged over the beta-beam cycle for the two different isotopes. For the PS the numbers are given at the end of accumulation.

The kinetic energy E_{kin} of the particles lost from the beam will be deposited in the vicinity of the beam line, mainly in magnetic elements and shielding. A representative number, which can be compared with other accelerator cases, is the time-averaged power loss per unit circumference of the machine

$$P_{\text{loss}}/l = \frac{\int_{t_{\text{cycle}}} \frac{dN(t)}{dt} E_{\text{kin}}(t) dt}{t_{\text{cycle}} * C_{\text{machine}}} \quad (1)$$

where t_{cycle} is the cycle time of the Beta-beam complex and C is the circumference of the machine.

POWER LOSSES

To some extent, the power losses of the Beta-beam can be compared with those expected for CNGS operation. It is assumed that the total energy deposition caused by an ion with mass number A is similar to that of A single protons in the momentum range above 100 MeV/u. However, losses are rather uniformly distributed around the circumference of the machines in the case of isotope decay, whereas for proton operation, most losses are associated with injection and extraction and occur at the relevant beam elements. Table 2 lists the ion losses of the Beta-beam scenario compared with the proton case of CNGS [7], where the two cases are comparable. It should be kept in mind that only decay losses of the Beta-beam scenario are taken into account here, whereas for CNGS, the total loss inventory is taken. Other losses known for stable ion operation have still to be studied and included

in the overall beam loss inventory for the Beta-beam scenario.

Table 2: Comparison of losses along the accelerator chain for CNGS and Beta-beam operation. ‘‘Ions’’ refer to protons in the CNGS case [7] and to the specific isotope of the Beta-beam.

Machine / beam		CNGS	Beta-beam	
		protons	${}^6\text{He}$	${}^{18}\text{Ne}$
RCS	Loss/cycle [ions]	-	$0.57 * 10^{12}$	$0.7 * 10^{11}$
	P_{loss} [W/m]	-	0.17	0.14
PS	Loss/cycle [ions]	$7.6 * 10^{12}$	$8.43 * 10^{12}$	$10.7 * 10^{11}$
	P_{loss} [W/m]	3.3	2.2	2.8
SPS	Loss/cycle [ions]	$3.8 * 10^{12}$	$0.53 * 10^{12}$	$0.6 * 10^{11}$
	P_{loss} [W/m]	0.25	0.4	0.25

The power loss, averaged over the PS circumference of 200 π m and the cycle time, is 2.2W/m for the ${}^6\text{He}$ case and 2.8W/m for the ${}^{18}\text{Ne}$ case.

LOSS DISTRIBUTION AND DYNAMIC VACUUM

The code StrahlSim [8] allows simulating the particle transport in an accelerator lattice including the effect of beta-decay providing information on the particle losses and the impact on the vacuum performance. In the beta-beam accelerator chain, the most demanding figures occur in the PS due to the accumulation procedure at flat bottom. Therefore the case of the PS is discussed in details here. The conclusions for all machines are summarized in the end.

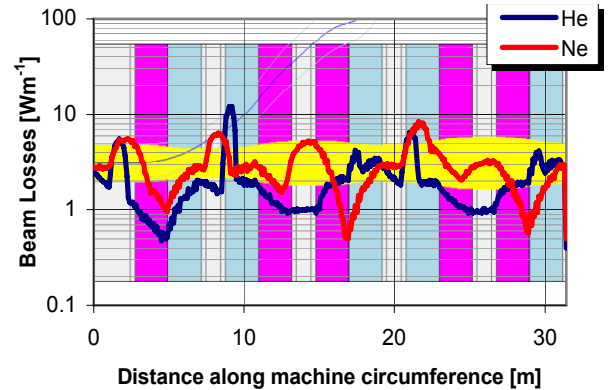


Figure 4: Loss distribution in terms of power deposition along one super cell of the PS machine for the case of ${}^6\text{He}$ (blue) and ${}^{18}\text{Ne}$ (red). The red and blue blocks indicate the position of the PS dipoles.

Loss Distribution

Figure 4 shows the loss distribution in terms of power averaged over an acceleration cycle of the daughter particles for the two cases of ${}^6\text{He}$ (blue) and ${}^{18}\text{Ne}$ (red). The losses are rather uniform, which means that no high performance cleaning scheme (i.e. absorbers) can be

installed. Moreover, the free space in the current PS machine is almost zero and does not allow the installation of additional objects like absorbers.

Dynamic Vacuum Simulation

Vacuum degradation is caused by desorption of molecules from the vacuum chamber. Two families of particles can cause desorption:

- Beam particles, which are lost due to
 - Change of magnetic rigidity either through charge state change or – which is equivalent in its effect by beta-decay
 - Deviated by Coulomb scattering
- Rest gas molecules, which were ionized by the beam and accelerated in its field.

The dominant effects for vacuum degradation are ionization of rest gas molecules due to the high beam currents (up to 3 Ampere) and the desorption by the impact of daughter particles of the beta-decay.

- First effect has a relatively small desorption yield ($\eta_{\text{restgas}} < 10$ [9]) per impinging particle, but enormous rate of ionized rest gas molecules involved.
- The second effect is relevant due to the energy of the particles lost, which result in a much higher desorption coefficient ($\eta_{\text{beam}} \approx 10^4$ [10]).

Figure 5 shows the dynamic vacuum behaviour for the two isotope cases. The yields for desorption by accelerated rest gas molecules is not very well known and has to be investigated experimentally. However, the upper limit of $\eta_{\text{beam}} = 10$ is not at all acceptable for a PS machine operation. With a fixed η_{restgas} the contribution of rest gas ionization can be estimated from figure 5, where the different values of $\eta_{\text{beam}} = 1$ and 5 are indicated. So, the vacuum degradation is dominated by the high beam currents. The PS beam chamber has been approximated by a 6m^3 large volume (residual gas pressure of 10^{-9} mbar) along the circumference of 200π m, where a total pumping power of 7600 l/s is assumed (equally distributed).

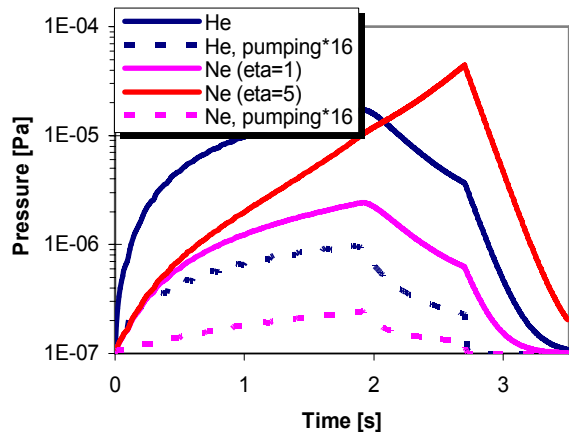


Figure 5: Evolution pressure for ${}^6\text{He}$ and ${}^{18}\text{Ne}$ in the PS.

Vacuum Improvements

Given the high number of ion requested for acceleration and a fixed residual gas pressure, the desorption caused

by rest gas ionization can be cured by an enhanced pumping power. As an example, it would require a 16 times higher pump rate than 7600 l/s to achieve a reasonable upper gas pressure of 10^{-8} mbar for the PS.

The vacuum degradation originating from the decay losses can as well be fought by optimizing the lattice and introducing a collimation system, which both require basically a new machine layout. Discussion of these possibilities is beyond the scope of this publication. An example for the design of a new machine in the PS class with an optimized lattice for transporting unstable ion beams can be found in [11].

The pressures in the RCS and SPS, however, were proven to remain within the nominal threshold of 10^{-8} mbar for safe continuous beta-beam operation. Neither of them have exponential growth in the pressure due to a higher energy and therefore a lower rate of beam loss per unit circumference in the SPS, and a lower intensity in the RCS.

CONCLUSION

It has been shown that beta beams can be produced to the annual rates desired by the neutrino physics community, but only if a higher pumping rate in the PS can be achieved. The issues of activation and the radiation hardness of accelerator components, particularly magnets, shall be investigated.

REFERENCES

- [1] P. Zucchelli, "A novel concept for a neutrino factory: the beta-beam", Phys. Let. B, 532 (2002) 166-172.
- [2] <http://www.eurisol.org>.
- [3] Parameter and Intensity Values, Version 2, July 2005, EURISOL DS/TASK12/TN-05-03.
- [4] J. Bouchez, M. Lindroos and M. Mezzetto, Beta-beams: Present design and expected performance, proc. Nufact 03, New York, 2003.
- [5] First design for the optics of the decay ring of the beta-beams, A. Chancé and J. Payet, EURISOL DS/TASK12/TN-06-05.
- [6] M. Benedikt, S. Hancock, A novel scheme for injection and stacking of radioactive ions at high energy, NIM A 550 (2005) 1–5.
- [7] M. Benedikt et al., Report of the High Intensity Protons Working Group, CERN-AB-2004-022-OP-RF.
- [8] C. Omet, P. Spiller, J. Stadlmann, "Simulation of Dynamic Vacuum Induced Beam Loss", These Proceedings.
- [9] O. Boine-Frankenheim, A. Krämer and G. Rumolo, "Estimations of beam lifetime in the SIS18", GSI internal report (2004).
- [10] E. Mustafin, O. Boine-Frankenheim, I. Hofmann, H. Reich-Sprenger and P. Spiller, "A theory of the beam loss-induced vacuum instability applied to the heavy-ion synchrotron SIS18", NIM A (2003), pp. 199-205
- [11] P. Spiller et al., proceedings of the Heavy Ion Fusion Conference, HIF04 Princeton (2004).